Mon. Not. R. astr. Soc. (1968) **140**, 387–402.

THE EVOLUTION OF PARTIALLY DEGENERATE HELIUM CORES

Peter P. Eggleton

(Received 1968 January 22)

Summary

Computations have been carried out on partially degenerate helium cores of red giants, evolving them from an initially isothermal state to a state where the temperature at some point is sufficiently high for helium to burn. Evolution to the helium flash was computed for various zero-age compositions ($X = 0{\cdot}65, 0{\cdot}9$; $Z = 0{\cdot}01, 0{\cdot}001, 0{\cdot}0001$), and the effect of different values for opacity and neutrino losses was considered. The possibility of nitrogen burning by α-particles was not included. This is reasonable for the lower two values of Z.

It is found that for stars on the verge of the helium flash $\log (L_{\text{bol}}/L_\odot)$ is in the range $3{\cdot}38 \pm 0{\cdot}1$ for all the above compositions. Although increasing the zero-age helium content from $0{\cdot}1$ to $0{\cdot}35$ decreases slightly the luminosity at the flash, the decrease appears to be too slight for it to be used as a criterion of the zero-age helium abundance in globular clusters. A preliminary examination of the seven globular cluster diagrams of Arp (1955), using the somewhat uncertain bolometric corrections for late giants, suggests that for the brightest star on each giant branch $\log (L_{\text{bol}}/L_\odot) \sim 3{\cdot}4 \pm 0{\cdot}2$.

1. *Introduction.* Once a low-mass red giant of between about $0{\cdot}9$ and 2 solar masses has developed a substantial inert partially degenerate helium core, the evolution of the core becomes largely independent of the part of the star outside the thin (with respect to mass) hydrogen burning shell surrounding the core. This result is based on the understanding that just outside the shell there is a region, at least a few temperature scale-heights in depth, which is in radiative equilibrium with an opacity occasioned mainly by Thomson scattering. The luminosity is very nearly constant in this region and so is the mass because the mean density here is much less, by a factor of 10^2 or more, than the mean density interior to the region. As a consequence of these facts it can be shown (Schwarzschild 1958; Hayashi, Hoshi & Sugimoto 1962) that equations (1)–(3) below hold at the edge of the core. Suffix *s* indicates values just interior to the hydrogen-burning shell and suffix *t* values just exterior, where they are different: pressure, temperature, radius and mass are (very nearly) continuous across the shell, while luminosity, composition, opacity and density are not.

$$\frac{G\mu_t\beta_s M_s}{R r_s t_s} = 4, \tag{1}$$

and

$$L_t = \frac{4\pi c G}{\kappa_t} M_s(1-\beta_s), \tag{2}$$

where

$$\frac{\beta_s}{1-\beta_s} = \frac{3R}{a\mu_t}\frac{\rho_t}{T_s^3} = \frac{3R}{a\mu_s}\frac{\rho_s}{T_s^3}, \tag{3}$$

In the theory from which these results are derived, composition, luminosity, β (the ratio of gas pressure to total pressure), mass and opacity are all assumed to be approximately constant for some way outside the shell. For a core in an early stage of development, say $M_s \sim 0 \cdot 2\, M_{\odot}$, these results are fairly accurate, but as the core develops, reaching $\sim 0 \cdot 5\, M_{\odot}$, they should improve considerably. A further, less accurate, equation can be obtained for the luminosity L_{H} resulting from hydrogen burning in the shell if the shell is assumed to be of virtually zero thickness, viz.

$$L_{\mathrm{H}} = L_t - L_s \doteqdot \frac{A X_{\mathrm{H}} X_{\mathrm{CNO}}}{\eta + 3} \rho_t{}^2 r_s{}^3 T_s{}^{\eta}, \tag{4}$$

where L_s is the luminosity just inside the shell, due to gravitational contraction of the core, and A, η are the ' constants ' in the approximate formula:

$$\epsilon_{\mathrm{H}} \doteqdot A X_{\mathrm{H}} X_{\mathrm{CNO}} \rho T^{\eta}, \tag{5}$$

for the energy generation by the CNO cycle. An improvement on this formula, where A, η are taken to be slowly-varying functions of temperature, is described in the next section. The rate at which the core mass increases is given by

$$L_{\mathrm{H}} = E_{\mathrm{H}} X_{\mathrm{H}} \frac{dM_s}{dt}, \tag{6}$$

where $E_{\mathrm{H}} = 6.10^{18}$ erg g^{-1}.

A correction can be made to these equations (Eggleton 1967) to allow for the fact that the shell has a finite thickness, in which pressure, temperature, luminosity, composition etc. all vary. This correction is based on the fact that equation (6) holds very accurately throughout the region where both X_{H} and L_{H} vary, as well as outside that region. With this correction, and after allowing for the fact that A, η in equation (4) vary slowly with temperature, the author feels that equation (4) should be not much less accurate than equations (1)–(3).

Two disadvantages of using these boundary conditions at the core's surface are obvious: firstly, it is difficult to assess just how accurate they are; and secondly, although they can be used to predict the luminosity of the star as it evolves up the giant branch (since this luminosity is almost entirely a result of hydrogen burning in the shell) they cannot say anything about the star's total radius or effective temperature and hence its colour. On the first point, it is encouraging to check the details of various red giant models that have been published (Iben 1967a; Härm & Schwarzschild 1964). They appear to show that the region of a giant just outside its shell does have the character assumed, and furthermore that the boundary conditions, equations (1)–(4), where they can be checked are reasonably accurate, and increase in accuracy as the core develops. On the second point, it has to be admitted that our knowledge of the physics of the cool, distended outer layers of red giants is not so good that the surface radius and effective temperature, even if obtained from detailed integrations of this region, can be considered reliable. Also, the corrections that have to be applied to luminosity and effective temperature to convert them to magnitude and colour are not sufficiently well known for the very late spectral types involved to make detailed calculations worth the labour involved. In the final section, we look for a means of comparing the present work with observations, using some criterion dependent only on the luminosity, and not on the effective temperature.

2. *The structure equations.* Since the temperature gradient in an inert helium core is slight, there is no convective transport of radiation. This applies until the core itself begins to burn, but in this work computations were stopped at that point, so that the heat transport is entirely radiative. Also the nitrogen burning reaction was ignored, so that the structure equations have the form

$$\frac{\partial p}{\partial m} = -\frac{Gm}{4\pi r^4}, \tag{7}$$

$$\frac{\partial r}{\partial m} = \frac{1}{4\pi r^2 \rho}, \tag{8}$$

$$\frac{\partial T}{\partial m} = -\frac{3\kappa L}{64\pi^2 acr^2 T^3} \tag{9}$$

$$\frac{\partial L}{\partial m} = -T\frac{\partial s}{\partial t} - \epsilon_\nu + \epsilon_{\mathrm{He}}. \tag{10}$$

Since the density and temperature in helium cores are such that the state of the electron gas varies from almost complete non-degeneracy at the surface to nearly relativistic degeneracy at the centre, the equation of state had to be somewhat complicated. In this work the equation of state was a patchwork of three different approximations to the Fermi-Dirac integrals which express pressure, density and entropy explicitly in terms of temperature and a degeneracy parameter ψ. For instance, the density is given by

$$\rho' = \mu_E \int_0^\infty \frac{x^2 dx}{e^{-\psi+E/T'}+1}, \qquad E = (1+x^2)^{1/2}-1, \tag{11}$$

where ρ' is the density in units of 3.10^6 g cm^{-3}, μ_E is the mean molecular weight per electron, x, E are the momentum and energy of an electron in relativistic units, and T' is the temperature in units of 6.10^9 degrees. Although with modern computers it is quite feasible to evaluate such integrals directly (Kippenhahn & Thomas 1964), or to store them in large tables as functions of ψ, T, the author considers it worthwhile to save a considerable fraction of computing time, with negligible loss of accuracy, by approximating these integrals with well-known analytic expressions (e.g. Chandrasekhar 1939). For density, we have (taking $\mu_E = 2$)

$$\rho' \doteqdot (2T')^{3/2}\left\{\int_0^\infty \frac{u^{1/2}du}{e^{u-\psi}+1} + \frac{5}{4}T'\int_0^\infty \frac{u^{3/2}du}{e^{u-\psi}+1}\right\} \tag{12}$$

for $T' \lesssim 0.1$, $\psi T' \lesssim 0.3$,

or

$$\rho' \doteqdot \sqrt{2\pi}\,(T')^{3/2}\,e^{\psi}\left\{1+\frac{e^{\psi}}{2^{3/2}}+\frac{15}{8}T'\left(1+\frac{e^{\psi}}{2^{5/2}}\right)\right\} \tag{13}$$

for $T' \lesssim 0.1$, $\psi \lesssim -1.5$

or

$$\rho' \doteqdot \frac{2}{3}x^3\left(1+\frac{\pi^2 T'^2}{2x^4}(1+2x^2)\right), \qquad x^2 = 2\psi T + \psi^2 T^2, \tag{14}$$

for $\psi \gtrsim 5$.

The approximate inequalities must be satisfied for about 1 per cent accuracy or better. In the present work the temperature was always much less than 6.10^8

degrees ($T' = 0 \cdot 1$), while ψ ranged from about -4 at the surface to at most 30 at the centre. Thus near the surface expression (13) can be used and over most of the interior expression (14) can be used; but in an intermediate zone neither is sufficiently accurate, and expression (12) must be used. In this expression the integrals are functions of ψ only, and the method used here was to find least-squares polynomials in ψ (of ninth order, though probably less would have done) which fitted the logarithms of the integrals in the range $|\psi| \lesssim 5$.

In view of the fact that equation (11), as well as similar equations for pressure and entropy, depends explicitly on ψ, T rather than on p, T, it is obviously more convenient to recast the equation of hydrostatic equilibrium (7) so that the variation of ψ rather than p is given, i.e.

$$\frac{\partial p}{\partial m} = \left(\frac{\partial p}{\partial \psi}\right)_T \frac{\partial \psi}{\partial m} + \left(\frac{\partial p}{\partial T}\right)_\psi \frac{\partial T}{\partial m} = -\frac{Gm}{4\pi r^4}. \tag{15}$$

The temperature gradient $\partial T/\partial m$ is given by equation (9), and the coefficients $\partial p/\partial \psi$, $\partial p/\partial T$ are themselves integrals such as equations (11) which can be evaluated in a similar way. Explicitly, these coefficients are obtained from the expression

$$p' = \frac{1}{3}\int_0^\infty \frac{x^4 dx/(1+x^2)^{1/2}}{e^{-\psi+E/T'}+1} + \frac{1}{\mu_I}\rho' T' + \frac{\pi^4}{45} T'^4, \tag{16}$$

where the unit for p' is $1 \cdot 5 . 10^{24}$ dyne cm^{-2}, μ_I is the mean molecular weight of the ions, and the other quantities are as in equation (11). The derivatives of pressure can be approximated analytically in the same way as for density. Similar approximations were also used for the entropy per unit mass, given by

$$s' = \frac{1}{3\rho' T'}\int_0^\infty \frac{d(x^3 E)}{e^{-\psi+E/T'}+1} - \frac{\psi}{\mu_E} + \frac{1}{\mu_I}\log\frac{T'^{3/2}}{\rho'} + \frac{4\pi^4}{45}\frac{T'^3}{\rho'}, \tag{17}$$

where s' is in units of $8 \cdot 4 . 10^7$ erg g^{-1}° K^{-1}.

The opacity was based on the work of Cox & Stewart (1965). Near the edge of the core the opacity is mainly electron scattering. Further in there is a region of free–free scattering, and this was calculated from a simple formula of Hayashi Hoshi & Sugimoto (1962), somewhat modified to reproduce more closely the results of Cox & Stewart. In the interior, electron conduction dominates and this was calculated from a simplification of Mestel's work (1950). Fig. 1 gives a comparison between the values used here and the tabulated values of Cox & Stewart for the Weigert IV mixture. For different Z, the free–free and conductive opacities were multiplied by $1 + 6Z$ (see later).

Neutrino losses were based on the results of Inman & Ruderman (1964) for plasma neutrinos. Their results are too large by a factor of four, and this was allowed for. A simple interpolation formula was used to represent their results in the range of temperatures and densities required here. A comparison of the results and the values used here is given in Fig. 2.

Although the hydrogen-burning rate ϵ_H is not required directly, the boundary condition (4) is obtained on the assumption that ϵ_H has a power-law dependence as in equation (5). This is not a good approximation over the complete range of shell temperatures (25 to $60 . 10^6$ degrees) encountered here. However, at any one time in the star's evolution as a red giant most of the hydrogen burning energy release occurs in a relatively narrow range of temperatures; typically, 90 p

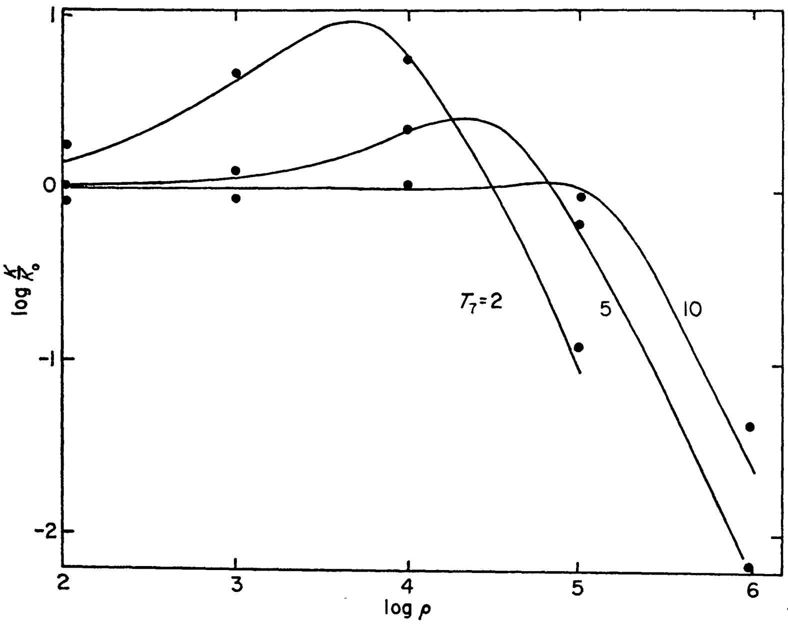

FIG. 1. *Comparison of the values of opacity used (continuous lines) and the values of Cox & Stewart* (1965) *(dots), for the Weigert IV mixture (Kippenhahn Population II with all hydrogen converted to helium).*

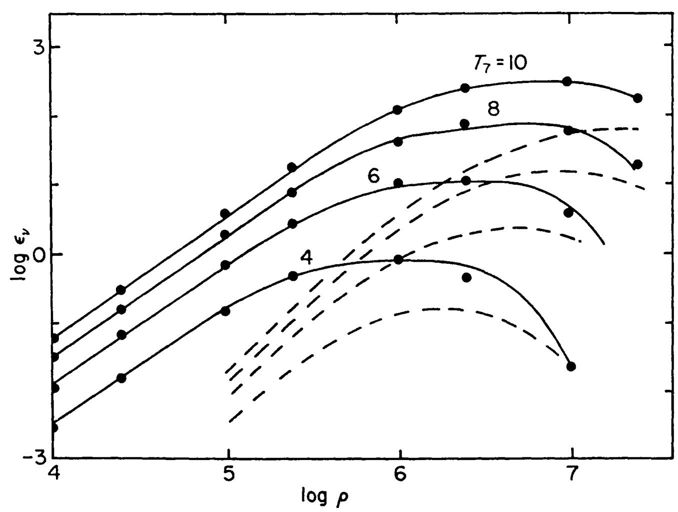

FIG. 2. *Comparison of the values of plasma neutrino energy losses used, multiplied by four (continuous lines) with some of the values of Inman & Ruderman* (1964) *(dots). The dashed lines represent neutrinos from longitudinal plasma oscillations (Adams, Ruderman & Woo* 1963).

cent of the star's luminosity arises in a temperature range of about 15 per cent. So it is reasonable to treat the quantities A, η in equation (5) as constant when we obtain equation (4), but they should be varied progressively as the shell temperature increases. Since ϵ_H is better represented by a formula

$$\epsilon_H = 10^{27.41} X_H X_{CNO} \rho T_7^{-2/3} \exp(-70 \cdot 69/T_7^{1/3}), \tag{18}$$

(Caughlan & Fowler 1962), we take A and η of equation (4) to be given by

$$\eta(T) \equiv \frac{\partial \log \epsilon_H}{\partial \log T} = -\frac{2}{3} + \frac{23 \cdot 56}{T_7^{1/3}}, \tag{19}$$

and

$$A(T) \equiv \frac{\epsilon_{\mathrm{H}}}{X_{\mathrm{H}} X_{\mathrm{CNO}} \rho T^{\eta}}. \tag{20}$$

Thus, if A, η are initially estimated, equations (1)–(4) can be solved for T_s, supposing (say) M_s, L_{H}, L_s are known, and then A, η recalculated from equations (18)–(20). The calculation can be repeated, and converges very rapidly.

The rate of the helium burning reaction was taken (Fowler & Hoyle 1964) as

$$\epsilon_{\mathrm{He}} = 10^{14\cdot 52} \rho^2 Y^3 T_7^{-3} \exp(-431\cdot 8/T_7), \tag{21}$$

with $Y = 1$, since computations were stopped before the helium abundance was significantly altered.

3. *The integration procedure.* We have mentioned that the hydrostatic equilibrium equation (7) was replaced by equation (15) which gives the quantity ψ rather than p. Further slight changes of variable were employed: instead of m, r, L the quantities $m^{2/3}$, r^2, $m^{-1/3} \log(1+L/L_{\odot})$ were used. In these variables all the gradients which appear on the right of the structure equations (7)–(10) are finite at the origin $m = 0$, so that there is the slight advantage that the equations do not have to be treated specially there. The slightly awkward form of the luminosity variable was determined partly by the fact that the luminosity varies much more steeply near the edge of the core than near the centre, so that a logarithmic variable, whose gradient is more nearly constant, seemed desirable and partly by the fact that in some of the core the luminosity is negative, though never as negative as $-L_{\odot}$.

The method of integration used was in a sense a compromise between the linearization procedure used by Henyey (Henyey, Wilets, Böhm, Leverrier & Levee 1959; Larson & Demargue 1964, etc.) for astrophysical problems, and the classical fitting-point method described by Schwarzschild (1958). In the former method, an initial guess is made in some way at the entire run of values of pressure, radius, temperature and luminosity through the star. From these guesses two separate estimates can be made of the gradients of these variables over one mesh space: the first by straightforward differencing, and the second by averaging the gradients at either end of the mesh space as obtained from the right-hand sides of the structure equations. Provided the initial guess is not unreasonably inaccurate, there should be linear relations between the errors in the guesses and the differences in the two estimates of gradients. These linear relations can be obtained explicitly by linearizing the structure equations about their exact solution, and using explicit formulae for the derivatives of the R.H.S.'s with respect to the dependent variables. They can also be obtained more simply by varying the guesses by small amounts and observing the variations they cause in the gradients: this procedure eliminates the need to differentiate some very complicated formulae analytically. The relations can be solved once the differences in the gradients have been computed, so that the errors in the guesses can be found, and much improved values obtained. The method can then be repeated if necessary until a satisfactory degree of convergence is obtained. The fitting-point method is not vastly different in essence. Instead of guessing values at all mesh-points, values are guessed only at the end-points and the structure equations are integrated from both ends to a suitable point in the middle. The values obtained at this point from the two integrations (or the gradients of these values, to make the analogy with the Henyey method closer) will not agree, but it is again assumed that there is a linear relation between the differences and the errors in the guesses. This relation cannot be obtained explicitly, unlike in the Henyey procedure, but it can be found by varying the guesses and observing the variation in the errors. Thus improved guesses can be obtained, provided the relation is indeed approximately linear.

The compromise used here was to make guesses only at a small selection of the mesh points, the two end ones and perhaps three intermediate ones. The equations could be integrated from these guessing points to intermediate fitting-points (four in this case). Once again, the errors at the fitting-points were assumed to be linearly related to the errors at the guessing points, and the relation was found by numerical differentiation. The advantage of this procedure over the simple fitting-point method is that since each integration is over a smaller portion of the range (an eighth instead of a half) there is more reason to believe that the relation will in fact be linear. It is well-known that the assumption of linearity in the simple procedure does break down in some models, as the integrations may diverge completely before reaching the fitting-point. As compared to the Henyey procedure we have the advantage of considerable programming simplicity, and very much less storage is required and the author feels that there may be a slight advantage in speed, as very much fewer linear equations have to be solved. There is possibly also an advantage in that it is not necessary for the right-hand sides of the structure equations to be continuous, let alone differentiable, functions of the variables. Since many quantities used in structure computations may be only piece-wise continuous, being obtained either by interpolation in a table or from a series of formulae applicable in different ranges, such a property is desirable. In a fitting-point procedure slight discontinuities in a function or its derivatives tend to get washed out over a reasonable range of integration, but in a linearizing procedure non-differentiability tends to pose extra problems.

The choice of the distribution of mesh-points in space and time was slightly complicated because the outer boundary of a helium core moves outwards in time, and because the variation of quantities such as pressure and entropy is extremely steep near the edge, though not in the centre. Suppose that the core mass (actually, $(\text{mass})^{2/3}$) is increased by 1 per cent per time-step; since the density varies by a factor of about 30 in the outermost 1 per cent it is necessary to put an additional 10 or 20 mesh-points here. But if the number of steps is not to become enormous in later models, it is necessary to discard some mesh-points further in. This was done in such a way that the number of mesh-points only increased by one for each time-step. The initial model in an evolutionary series usually had about 80 mesh-points, distributed mainly near the surface, and the final model about 130.

Another complication resulting from the outward movement of the boundary arises because in two consecutive models the later and heavier model has mesh-points in its outermost 1 per cent for which there are no corresponding mesh-points in the earlier model. Thus the term $(\partial s/\partial t)_m$ cannot be found in this region by differencing between successive models. In any event such a procedure would not be reliable with the large time-steps used here, since $\partial^2 s/\partial t^2$ is very large in the outer part of the core so that the first difference of entropy is not a reliable measure of its first derivative. In this region the assumption was therefore made

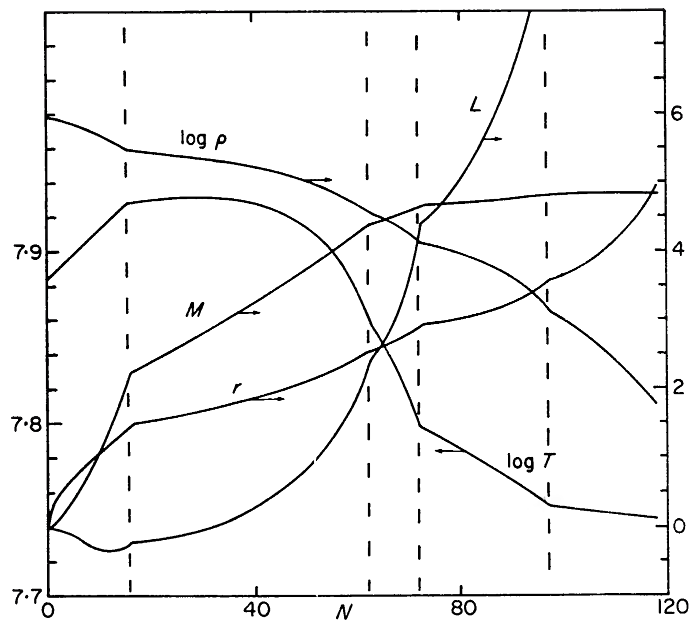

FIG. 3. *Structural details of a model helium core corresponding to a zero-age composition* $X = 0{\cdot}65$, $Z = 0{\cdot}001$, *just prior to the helium flash Mass is in units of* $0{\cdot}1\ M_\odot$, *luminosity in units of* $L_\odot$, *and radius in units of* 4.10^8 *cm. The abscissa is the number of the mesh-point; the length of mass-step was changed by a factor of 2 or 5 at each of the dashed vertical lines.*

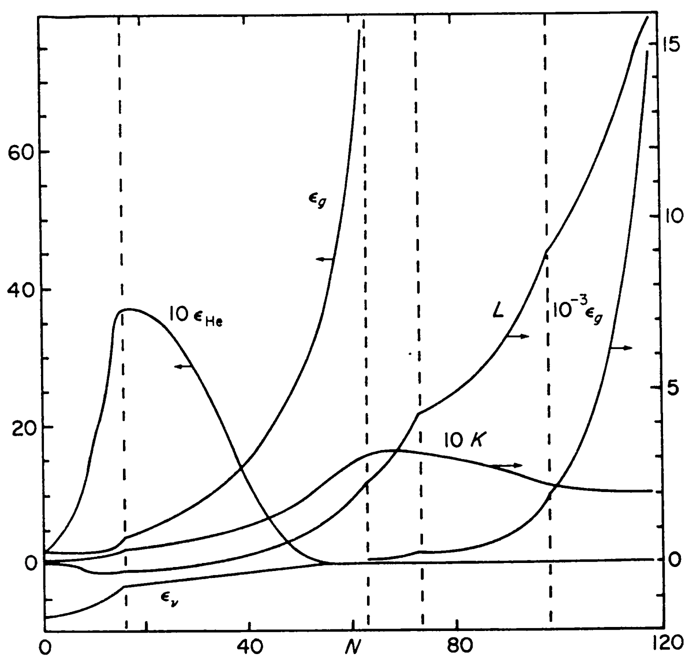

FIG. 4. *More structural details of the same model as in Fig. 3. Luminosity is in solar units, energy generation and opacity in cgs units.*

that the entropy distribution is very nearly a function only of distance (with respect to mass) from the core's edge, i.e. that

$$s = s(m - M_s(t)), \tag{22}$$

so that

$$\left(\frac{\partial s}{\partial t}\right)_m = -\left(\frac{\partial s}{\partial m}\right)_t \frac{dM_s}{dt}. \tag{23}$$

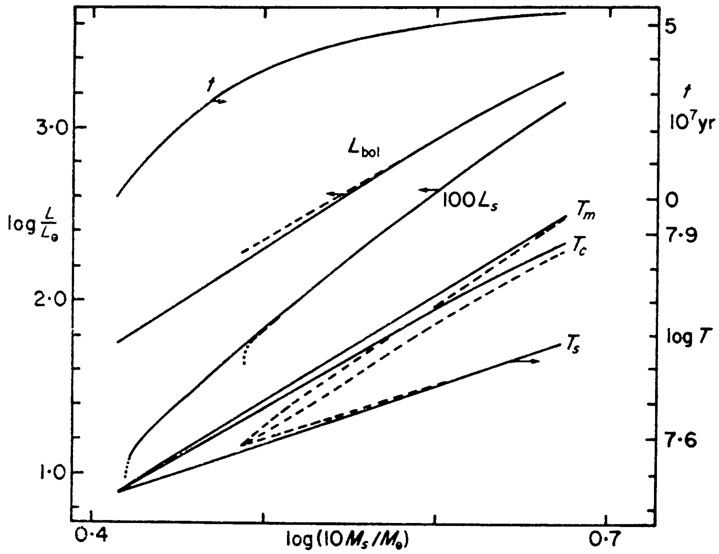

FIG. 5. *Evolutionary details of two helium cores with the same zero-age composition $X = 0 \cdot 65$, $Z = 0 \cdot 001$, but starting from isothermal configurations at different masses. T_m, T_c and T_s are the maximum, central and surface temperatures of the core, L_s the core luminosity and L_{bol} the luminosity of core plus shell (the same as L_t, see text). The central temperature converges less rapidly than the other two because most of the heat comes from contraction of the outer layers and therefore reaches the centre last.*

A similar procedure has been used, by other workers and the author, for the distribution of chemical composition near a nuclear burning shell (Härm & Schwarzschild 1966; Iben 1967b; Thomas 1967 & Eggleton 1967), and for gravitational energy release (Eggleton 1966; Weigert 1966; Thomas 1967). This formula allows one to calculate $\partial s/\partial t$ in the region where there are no mesh-points in the previous model and in fact can be used rather further in, up to about 2 per cent of the core's mass, since it is more reliable than differencing. In Fig. 4 showing

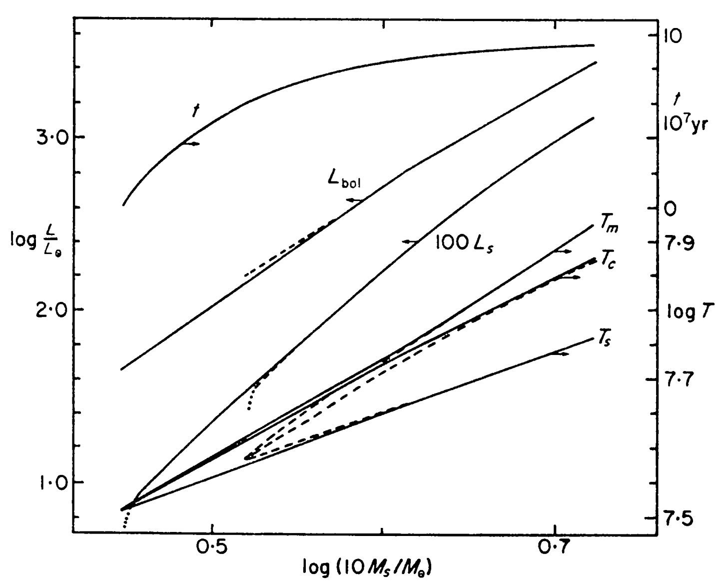

FIG. 6. *Similar to Fig. 5 but for a zero-age composition of $X = 0 \cdot 9$, $Z = 0 \cdot 001$. The convergence is more rapid partly because the temperature difference in the core is less, for the same core mass.*

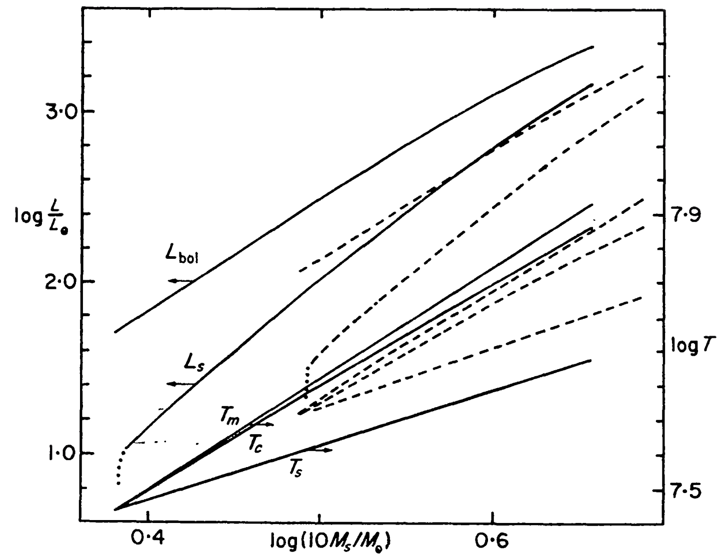

FIG. 7. *Evolutionary details of two helium cores with zero-age compositions $X = 0{\cdot}65$, $Z = 0{\cdot}01$ (continuous line) and $Z = 0{\cdot}0001$ (dashed line). T_m, T_c and T_s are the maximum, central and surface temperatures in the core, L_s the luminosity of the core, allowing for neutrino losses, and L_{bol} is the luminosity of core plus shell.*

the structure of a typical model a slight discontinuity is observed in $\epsilon_g \equiv -T\,\partial s/\partial t$ at the point ($N = 92$) where the formula (23) takes over from differencing.

In all the evolutionary sequences presented here the sequence was started with an isothermal model. Although an inert helium core will probably never pass through a completely isothermal state, it is reasonable to suppose that in its late phase of evolution it will have forgotten the details of a nearly isothermal early stage, so that the exact starting model should not be important. This is illustrated in Figs 5 and 6, where evolutionary sequences for the same zero-age chemical composition, but for different initial core masses, are compared. It will be seen that the sequences converge quite strongly during the later stages of

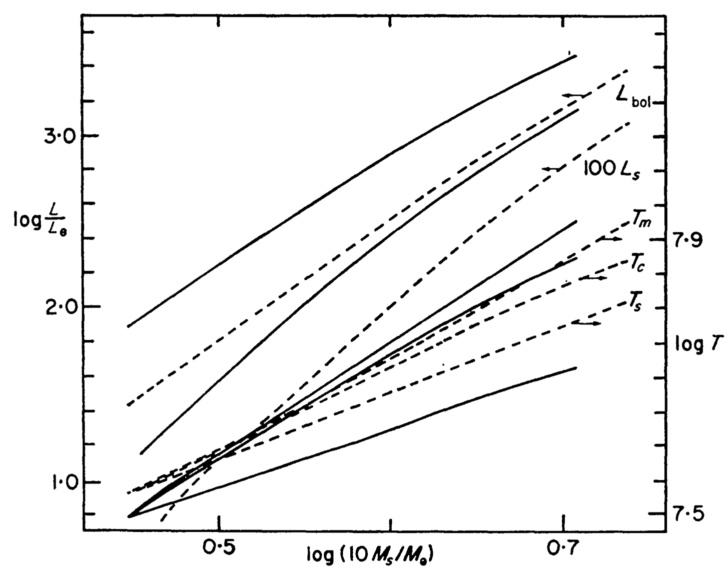

FIG. 8. *Similar to Fig. 7, but for zero-age compositions $X = 0{\cdot}9$, $Z = 0{\cdot}01$ (continuous lines) and $Z = 0{\cdot}0001$ (dashed lines).*

evolution, although they are considerably different at an early stage. This suggests that the core does largely forget its initial state by the time it reaches the helium flash.

4. *Results*. Evolutionary sequences were computed for six different compositions of the material outside the core: $X = 0{\cdot}65$ and $0{\cdot}9$; $Z = 0{\cdot}01$, $0{\cdot}001$ and $0{\cdot}0001$. In each case it was assumed that $X_{\mathrm{CNO}} = 0{\cdot}6\ Z$. Each sequence required 30 to 60 min of computing time on an IBM 360/44, although later calculations using fewer mesh points took only 20 min, with negligible loss of accuracy. Structural details of a model just prior to the flash are given in Table I and Figs 3 and 4. Details of evolutionary sequences are given in Tables II–VII and Figs 5–8.

A comparison of the results of the present work for the model $X = 0{\cdot}9$, $Z = 0{\cdot}001$ with the work of Härm & Schwarzschild (1966) shows that our model reaches the helium flash at lower mass and total luminosity. This is probably a result of the onset of relativistically degenerate conditions near the centre in the later stages, leading to more rapid contraction and heating up. The effect of

TABLE I

Structural details of a partially degenerate helium core shortly before the flash. The zero-age composition was $X = 0{\cdot}9$, $Z = 0{\cdot}001$. Of the 119 mesh-points 28 are tabulated, at equal intervals of $(mass)^{2/3}$. The detached integer gives the power of ten by which the entry to its left must be multiplied

$10\ m/M_\odot$	$\log r$	$\log \rho$	$\log T$	$\dfrac{L}{L_\odot}$	$10\ \kappa$	ϵ_g		$-\epsilon_\nu$		ϵ_{He}	
0·0	—	6·115	7·861	0·0	0·025	2·75	0	−7·33	0	2·07	−2
0·037	8·048	6·095	7·863	−0·009	0·027	2·78	0	−7·35	0	2·44	−2
0·104	8·203	6·073	7·866	−0·025	0·030	2·84	0	−7·37	0	2·92	−2
0·192	8·295	6·051	7·868	−0·046	0·033	2·88	0	−7·36	0	3·48	−2
0·295	8·362	6·029	7·870	−0·070	0·036	2·94	0	−7·34	0	4·17	−2
0·413	8·415	6·006	7·872	−0·096	0·040	3·00	0	−7·29	0	5·01	−2
0·542	8·459	5·982	7·875	−0·125	0·045	3·07	0	−7·22	0	6·05	−2
0·683	8·497	5·956	7·877	−0·154	0·050	3·15	0	−7·12	0	7·31	−2
0·835	8·531	5·930	7·880	−0·185	0·056	3·25	0	−6·99	0	8·86	−2
0·996	8·562	5·902	7·882	−0·214	0·064	3·36	0	−6·82	0	1·07	−1
1·167	8·590	5·873	7·885	−0·243	0·072	3·50	0	−6·61	0	1·30	−1
1·346	8·167	5·843	7·887	−0·269	0·083	3·67	0	−6·36	0	1·57	−1
1·534	8·642	5·810	7·890	−0·291	0·096	3·87	0	−6·06	0	1·89	−1
1·729	8·665	5·776	7·893	−0·309	0·112	4·12	0	−5·72	0	2·26	−1
1·933	8·688	5·739	7·896	−0·319	0·131	4·43	0	−5·34	0	2·67	−1
2·143	8·710	5·700	7·899	−0·321	0·156	4·83	0	−4·91	0	3·12	−1
2·361	8·732	5·657	7·901	−0·313	0·188	5·34	0	−4·44	0	3·49	−1
2·586	8·753	5·612	7·904	−0·291	0·228	5·97	0	−3·95	0	3·81	−1
2·818	8·774	5·561	7·906	−0·254	0·282	6·80	0	−3·43	0	3·96	−1
3·056	8·795	5·506	7·908	−0·197	0·356	7·90	0	−2·90	0	3·86	−1
3·300	8·817	5·443	7·910	−0·115	0·457	9·38	0	−2·37	0	3·43	−1
3·551	8·839	5·371	7·910	−0·002	0·603	1·15	1	−1·86	0	2·65	−1
3·807	8·862	5·287	7·909	0·154	0·819	1·44	1	−1·37	0	1·64	−1
4·070	8·887	5·185	7·906	0·368	1·145	1·89	1	−9·31	−1	7·01	−2
4·338	8·915	5·055	7·898	0·669	1·654	2·59	1	−5·55	−1	1·54	−2
4·612	8·947	4·875	7·881	1·121	2·442	3·99	1	−2·62	−1	8·20	−3
4·891	8·992	4·564	7·842	1·978	3·290	8·70	1	−7·12	−2	1·20	−6
5·176	9·217	1·794	7·755	11·792	1·971	1·96	4	−5·02	−3	7·08	−18

TABLE II

Evolution of a partially degenerate helium core towards the flash.
Zero-age composition $X = 0\cdot65$, $Z = 0\cdot01$

Model number	$\frac{10\,M_s}{M_\odot}$	$\log \frac{L_t}{L_\odot}$	$\log \rho_s$	$\log T_s$	$\log r_s$	$\log \frac{L_s}{L_\odot}$	β_s	$\log \rho_c$	$\log T_c$	$\log T_m$	$\log t$	f
1	2·40	1·71	2·31	7·47	9·31	$-\infty$	0·99	5·27	7·47	7·47	$-\infty$	−
6	2·58	1·91	2·22	7·49	9·32	−0·73	0·99	5·34	7·52	7·52	7·27	−
11	2·77	2·11	2·12	7·52	9·32	−0·46	0·99	5·40	7·56	7·57	7·48	−
16	2·96	2·31	2·03	7·54	9·33	−0·21	0·98	5·46	7·61	7·62	7·58	−
21	3·16	2·49	1·95	7·56	9·33	0·02	0·98	5·52	7·65	7·66	7·63	−
26	3·36	2·66	1·88	7·59	9·33	0·24	0·97	5·58	7·69	7·70	7·67	−
31	3·56	2·81	1·81	7·61	9·33	0·43	0·96	5·63	7·73	7·74	7·69	−9
36	3·76	2·93	1·76	7·62	9·33	0·58	0·94	5·68	7·76	7·78	7·70	−7
41	3·98	3·09	1·70	7·65	9·32	0·78	0·93	5·74	7·80	7·82	7·71	−5
46	4·19	3·21	1·65	7·66	9·32	0·94	0·91	5·80	7·83	7·86	7·72	−3
51	4·41	3·32	1·62	7·68	9·31	1·08	0·89	5·85	7·86	7·90	7·73	−1
54	4·53	3·38	1·60	7·69	9·31	1·16	0·87	5·88	7·88	7·92	7·73	−0

Suffix s refers to just inside the hydrogen burning shell, suffix t to just outside, suffix c the core's centre and suffix m to the maximum value. The quantity f is the value of log ($\epsilon_{He}/\epsilon_{to}$ at the point where ϵ_{He} is a maximum; usually when this became greater than about $-0\cdot5$ method of computation broke down, indicating the beginning of the flash.

TABLE III

Zero-age composition $X = 0\cdot65$, $Z = 0\cdot001$

Model number	$\frac{10\,M_s}{M_\odot}$	$\log \frac{L_t}{L_\odot}$	$\log \rho_s$	$\log T_s$	$\log r_s$	$\log \frac{L_s}{L_\odot}$	β_s	$\log \rho_c$	$\log T_c$	$\log T_m$	$\log t$	f
1	2·59	1·75	2·46	7·52	9·29	$-\infty$	0·99	5·35	7·52	7·52	$-\infty$	−
6	2·79	1·95	2·36	7·54	9·30	−0·65	0·99	5·41	7·57	7·57	7·27	−
11	3·00	2·15	2·27	7·57	9·30	−0·38	0·99	5·48	7·61	7·62	7·48	−
16	3·21	2·35	2·19	7·59	9·30	−0·13	0·98	5·54	7·66	7·66	7·58	−
21	3·42	2·53	2·11	7·62	9·30	0·10	0·98	5·61	7·69	7·70	7·64	−
26	3·63	2·70	2·04	7·64	9·30	0·32	0·97	5·67	7·73	7·74	7·67	−
31	3·85	2·85	1·97	7·66	9·30	0·52	0·95	5·73	7·77	7·78	7·69	−
36	4·08	3·00	1·92	7·69	9·30	0·70	0·94	5·78	7·80	7·82	7·71	−
41	4·31	3·13	1·87	7·71	9·29	0·87	0·92	5·84	7·83	7·86	7·72	−
46	4·54	3·25	1·82	7·72	9·29	1·03	0·90	5·90	7·86	7·90	7·73	−
49	4·68	3·32	1·80	7·73	9·29	1·11	0·89	5·93	7·88	7·92	7·73	−

See comments on Table II.

TABLE IV

Zero-age composition $X = 0\cdot65$, $Z = 0\cdot0001$

Model number	$\frac{10\,M_s}{M_\odot}$	$\log \frac{L_t}{L_\odot}$	$\log \beta$	$\log T_s$	$\log r_s$	$\log \frac{L_s}{L_\odot}$	β_s	$\log \rho_c$	$\log T_m$	$\log T_m$	$\log t$	
1	3·07	2·06	2·49	7·61	9·27	$-\infty$	0·99	5·52	7·61	7·61	$-\infty$	·
6	3·30	2·26	2·40	7·63	9·28	−0·23	0·99	5·59	7·65	7·66	7·03	·
11	3·54	2·46	2·32	7·66	9·28	0·03	0·98	5·65	7·70	7·71	7·25	·
16	3·79	2·64	2·24	7·69	9·28	0·27	0·97	5·72	7·74	7·76	7·35	−
21	4·04	2·81	2·17	7·71	9·28	0·49	0·96	5·79	7·78	7·80	7·40	−
26	4·29	2·97	2·11	7·74	9·27	0·70	0·95	5·58	7·82	7·84	7·44	−
31	4·55	3·12	2·06	7·76	9·27	0·89	0·93	5·92	7·85	7·88	7·46	−
36	4·82	3·25	2·01	7·78	9·26	1·06	0·91	5·98	7·88	7·92	7·48	−
37	4·87	3·28	2·01	7·78	9·26	1·09	0·91	5·99	7·88	7·93	7·48	

See comments on Table II.

TABLE V

Zero-age composition $X = 0.9$, $Z = 0.01$

Model number	$10\,M_s/M_\odot$	$\log L_t/L_\odot$	$\log \rho_s$	$\log T_s$	$\log r_s$	$\log L_s/L_\odot$	β_s	$\log \rho_c$	$\log T_c$	$\log T_m$	$\log t$	f
1	2.40	1.36	2.48	7.43	9.27	$-\infty$	1.00	5.30	7.43	7.43	$-\infty$	—
6	2.58	1.54	2.39	7.45	9.27	−1.30	1.00	5.36	7.47	7.47	7.67	—
11	2.77	1.81	2.27	7.48	9.28	−0.94	0.99	5.44	7.52	7.52	7.95	—
16	2.96	2.03	2.17	7.51	9.28	−0.67	0.99	5.50	7.56	7.56	8.04	—
21	3.16	2.23	2.07	7.54	9.28	−0.42	0.99	5.57	7.60	7.60	8.09	—
26	3.36	2.41	1.99	7.56	9.28	−0.19	0.98	5.63	7.63	7.64	8.12	—
31	3.56	2.58	1.91	7.59	9.27	0.03	0.97	5.69	7.67	7.68	8.14	—
36	3.76	2.75	1.85	7.61	9.27	0.23	0.96	5.75	7.70	7.71	8.15	—
41	3.98	2.89	1.78	7.63	9.27	0.42	0.95	5.80	7.74	7.75	8.16	−9.3
46	4.19	3.03	1.73	7.65	9.26	0.59	0.93	5.86	7.77	7.79	8.17	−7.0
51	4.41	3.15	1.68	7.67	9.26	0.75	0.91	5.91	7.80	7.83	8.17	−5.0
56	4.63	3.27	1.64	7.68	9.25	0.89	0.89	5.97	7.83	7.86	8.17	−3.3
61	4.86	3.37	1.61	7.70	9.25	1.03	0.87	6.02	7.86	7.89	8.18	−1.7
65	5.04	3.45	1.59	7.71	9.24	1.13	0.85	6.06	7.87	7.92	8.18	−0.5

See comments on Table II.

TABLE VI

Zero-age composition $X = 0.9$, $Z = 0.001$

Model number	$10\,M_s/M_\odot$	$\log L_t/L_\odot$	$\log \rho_s$	$\log T_s$	$\log r_s$	$\log L_s/L_\odot$	β_s	$\log \rho_c$	$\log T_c$	$\log T_m$	$\log t$	f
1	3.30	2.20	2.26	7.58	9.25	$-\infty$	0.99	5.64	7.58	7.58	$-\infty$	—
6	3.55	2.40	2.17	7.61	9.25	−0.20	0.98	5.71	7.63	7.65	7.06	—
11	3.81	2.60	2.08	7.64	9.25	0.07	0.97	5.78	7.68	7.70	7.28	—
16	4.07	2.79	2.01	7.66	9.24	0.31	0.96	5.85	7.72	7.74	7.38	—
21	4.34	2.96	1.94	7.69	9.24	0.53	0.94	5.91	7.76	7.79	7.43	−7.4
26	4.61	3.11	1.88	7.71	9.23	0.73	0.92	5.98	7.80	7.83	7.47	−4.9
31	4.89	3.25	1.83	7.73	9.23	0.91	0.90	6.05	7.83	7.87	7.49	−2.9
36	5.18	3.38	1.79	7.76	9.22	1.07	0.87	6.11	7.86	7.91	7.51	−1.0
39	5.35	3.45	1.77	7.77	9.21	1.16	0.85	6.15	7.88	7.94	7.52	0.1

See comments on Table II.

TABLE VII

Zero-age composition $X = 0.9$, $Z = 0.0001$

Model number	$10\,M_s/M_\odot$	$\log L_t/L_\odot$	$\log \rho_s$	$\log T_s$	$\log r_s$	$\log L_s/L_\odot$	β_s	$\log \rho^2$	$\log T_c$	$\log T_m$	$\log t$	f
1	2.80	1.43	2.77	7.53	9.23	$-\infty$	1.00	5.45	7.53	7.53	$-\infty$	—
6	3.01	1.66	2.67	7.56	9.24	−1.10	1.00	5.52	7.57	7.57	7.74	—
11	3.23	1.88	2.57	7.59	9.24	−0.81	0.99	5.59	7.61	7.61	7.95	—
16	3.45	2.09	2.48	7.62	9.23	−0.54	0.99	5.66	7.64	7.64	8.04	—
21	3.68	2.29	2.40	7.64	9.23	−0.29	0.99	5.73	7.67	7.68	8.09	—
26	3.91	2.48	2.32	7.67	9.23	−0.05	0.98	5.80	7.71	7.72	8.12	—
31	4.15	2.65	2.25	7.70	9.23	0.17	0.97	5.86	7.74	7.75	8.14	−9.6
36	4.39	2.81	2.18	7.72	9.22	0.37	0.96	5.93	7.77	7.79	8.15	−7.1
41	4.64	2.96	2.13	7.74	9.22	0.56	0.94	5.99	7.79	7.82	8.16	−5.2
46	4.89	3.10	2.08	7.76	9.21	0.74	0.93	6.05	7.82	7.86	8.17	−3.6
51	5.14	3.22	2.04	7.78	9.20	0.90	0.91	6.12	7.84	7.89	8.17	−2.0
56	5.40	3.34	2.00	7.80	9.20	1.05	0.89	6.18	7.87	7.92	8.18	−0.5
58	5.51	3.38	1.99	7.81	9.19	1.11	0.88	6.20	7.87	7.94	8.18	0.1

See comments on Table II.

varying X or Z is qualitatively much as one would expect. Increasing Z at constant Y increases the shell luminosity for the same core mass, temperature being determined almost entirely by the core mass and radius which are largely independent of composition. Thus the core grows faster and reaches the flash at a lower mass. For fixed Z as Y increases the core mass grows faster at nearly the same luminosity, mass and temperature, so that once again the flash is reached sooner. For low helium density this tendency is reinforced by the fact that higher mass implies higher density and higher neutrino losses, thus slowing down the evolution even more. However, this is to some extent countered by the onset of relativistic degeneracy, which accelerates contraction and heating up. The metal abundance Z also affects evolution slightly through increasing free–free scattering by a factor $\Sigma X_i B_i^2/A_i$ where X_i is the mass-abundance of the ith nuclide, B_i is its ionic charge and A_i is its atomic weight. This factor $\sim 1+6Z$ for helium plus metals. The same factor multiplies electron conductive opacity when this is dominant.

The significance of plasma neutrino losses, and of free–free scattering, in the evolution to the helium flash was considered by separate calculations with (a) neutrino losses ignored, (b) neutrino losses doubled, (c) free–free scattering halved, (d) free–free scattering doubled. The effects of these variations are summarized in Table VIII. Once again the results are qualitatively what one would expect. Increasing the neutrino losses delays the flash further and also pushes the site of the flash further out in the star. Ignoring the neutrinos hastens the flash, and sites it at the centre. However, there is nonetheless a slight increase in temperature going outwards from the centre; no doubt for more helium- or metal-rish stars this increase could be larger, leading to a non-central flash even without the assistance of neutrinos. If the opacity is taken to be larger than the standard values used the flash is again accelerated, because more heat is retained in the core and the site of the flash is again moved outward, because most of this heat comes from the outer layers. The position of the helium flash in the core is of interest because presumably a flash in the deep interior of the core is a much

TABLE VIII

Conditions just before the helium flash

X	Z	$\frac{10\,M_s}{M_\odot}$	$\log \frac{L_t}{L_\odot}$	$\log \rho_s$	$\log T_s$	$\log r_s$	$\log \frac{L_s}{L_\odot}$	β_s	$\log \rho_c$	$\log T_c$	$\log T_m$	q
0·65	0·01	4·53	3·38	1·60	7·69	9·31	1·16	0·87	5·88	7·88	7·92	0·
0·65	0·001	4·68	3·32	1·80	7·73	9·29	1·11	0·89	5·93	7·88	7·92	0·
0·65	0·0001	4·87	3·28	2·01	7·78	9·26	1·09	0·91	5·99	7·88	7·93	0·
0·90	0·01	5·04	3·45	1·59	7·71	9·24	1·13	0·85	6·06	7·87	7·92	0·
0·90	0·001	5·35	3·45	1·77	7·77	9·21	1·16	0·85	6·15	7·88	7·94	0·
0·90	0·0001	5·51	3·38	1·99	7·81	9·19	1·11	0·88	6·20	7·87	7·94	0·
0·90 a	0·001	4·95	3·27	1·83	7·74	9·23	0·93	0·90	6·04	7·90	7·91	0·
0·90 b	0·001	5·46	3·50	1·76	7·78	9·20	1·23	0·84	6·20	7·84	7·94	0·
0·90 c	0·001	5·52	3·53	1·75	7·78	9·20	1·28	0·83	6·21	7·90	7·93	0·
0·90 d	0·001	5·12	3·33	1·81	7·74	9·23	1·00	0·88	6·09	7·85	7·94	0·

Suffix s refers to just inside the hydrogen burning shell, suffix t to just outside, suffix c to t core's centre and suffix m to the maximum value. The quantity q is the mass-fraction in the c at which helium burning is a maximum. Since each line in this table describes the last mo in its sequence to converge, some models may be more pre-flash than others, leading to a f amount of scatter. (a) No neutrino losses, (b) neutrino losses doubled, (c) free–free and conduct opacities halved, (d) free–free and conductive opacities doubled.

more dramatic affairs than a flash near the surface and this may affect the possibility of products of the flash becoming mixed with the rest of the star. The author hopes to adapt the method used here to follow various models through the flash and check the possibility of mixing.

Attempts to relate the above work to observations on the giant branches of cluster diagrams are at present in progress. Since bolometric luminosities (which we take to be the same as the quantity L_t of equations (2) and (4) and Tables II–VIII, i.e. we ignore any absorption or release of internal energy in the outer part of the star) are the main results of this work which are capable of observational measurement, the following result may be significant. It appears that over the total range of composition considered here ($X = 0{\cdot}65$, $0{\cdot}9$; $Z = 0{\cdot}01$, $0{\cdot}001$, $0{\cdot}0001$) the bolometric luminosity of a star on the verge of the helium flash lies in a rather narrow range $\log(L_{\mathrm{bol}}/L_\odot) = 3{\cdot}38 \pm 0{\cdot}1$. A crude check of the colour-magnitude diagrams given by Arp (1955) of the seven globular clusters M3, M5, M13, M10, M92, M15 and M2, using the bolometric corrections given by Harris (1963) shows that the brightest star on the giant branch of each cluster (excluding two long-period variables) lies in the range

$$\log(L_{\mathrm{bol}}/L_\odot) = 3{\cdot}45 \pm 0{\cdot}1.$$

Several approximations were made in this quick calculation: the bolometric corrections are for V, B–V while the cluster diagrams are in terms of m_{pv}, m_{pg}; the bolometric corrections are given up to B–$V = 1{\cdot}5$ but one cluster ($M3$) extends up to $1{\cdot}6$; the corrections are for luminosity class III although the brightest stars are more likely to be luminosity class II; the RR Lyrae gap was taken by Arp to be at $M_{pv} = 0{\cdot}0$, a value which may not be correct; no allowance was made for the possible effect of metal deficiency in globular clusters on the bolometric correction. Using Johnson's (1966) bolometric corrections for classes I and III, taking their mean to represent class II, we get a slightly lower value of $3{\cdot}33 \pm 0{\cdot}1$. Thus our present estimate, which we hope to improve at a later date, for the bolometric luminosity of the brightest red giant in the seven globular clusters is $\log(L_{\mathrm{bol}}/L_\odot) = 3{\cdot}4 \pm 0{\cdot}2$. Because stars near the flash are evolving very rapidly compared with stars lower down the giant branch, the brightest red giant in a cluster may still be some way from the flash, so that the above estimate can only be a lower limit to the bolometric luminosity at which the flash occurs. A further complication is the possibility that the brightest red giants may be post-helium-flash stars which have travelled to the horizontal branch and returned up the giant branch.

The author had hoped that the present work might give some indication, however weak, of the zero-age helium content of globular clusters. However, it seems that our theoretical work gives too small a variation of maximum luminosity and the observations too large an uncertainty at the present time, for this purpose.

Institute of Theoretical Astronomy,
Madingley Road,
Cambridge.
1968 *January.*

References

Adams, B., Ruderman, M. A. & Woo, C., 1963. *Phys. Rev.*, **129,** 1383.
Arp, H. C., 1955. *Astrophys. J.*, **60,** 317.
Caughlan, G. R. & Fowler, W. A., 1962. *Astrophys. J.*, **136,** 453.

Chandrasekhar, S., 1939. *Introduction to the Study of Stellar Structure*, University of Chicago Press.
Cox, A. N. & Stewart, J. N., 1965. *Astrophys. J., Suppl. Ser.*, **94**, 22.
Eggleton, P. P., 1966. Ph.D. Thesis, University of Cambridge.
Eggleton, P. P., 1967. *Mon. Not. R. astr. Soc.*, **135**, 243.
Fowler, W. A. & Hoyle, F., 1964. *Astrophys. J., Suppl. Ser.*, **91**, 201.
Härm, R. & Schwarzschild, M., 1964. *Astrophys. J.*, **139**, 594.
Härm, R. & Schwarzschild, M., 1966. *Astrophys. J.*, **145**, 496.
Harris, D. L., 1963. *Basic Astronomical Data*, ed. by K. Aa. Strand, University of Chicago Press.
Hayashi, C., Hoshi, R. & Sugimoto, D., 1962. *Prog. theor. Phys., Suppl.*, **12**, 1.
Henyey, L. G., Wilets, L., Böhm, K., Leverrier, R. & Levee, R. D., 1959. *Astrophys. J.*, **129**, 628.
Iben, I., 1967a. *Astrophys. J.*, **147**, 624.
Iben, I., 1967b. *Astrophys. J.*, **147**, 650.
Inman, C. L. & Ruderman, M. A., 1964. *Astrophys. J.*, **140**, 1025.
Johnson, H. L., 1966. *Ann. Rev. Astr. Astrophys.*, **4**, 193.
Kippenhahn, R. & Thomas, H.-C., 1964, *Z. Astrophys.*, **60**, 19.
Larson, R. B. & Demarque, P. R., 1964. *Astrophys. J.*, **140**, 524.
Mestel, L., 1950. *Proc. Camb. phil. Soc., Math. Phys. Sci.*, **46**, 331.
Schwarzschild, M., 1958. *Structure and Evolution of the Stars*, Princeton University Press.
Thomas, H.-C., 1967. *Z. Astrophys.*, **67**, 420.
Weigert, A., 1966. *Z. Astrophys.*, **64**, 395.